Proceedings of ICONE 8
8th International Conference on Nuclear Engineering
April 2-6, 2000, Baltimore, MD USA

ICONE-8568

TWO-PHASE FLOW STABILITY IN LOW PRESSURE PARALLEL VERTICAL HEATED ANNULI

N.K. Popov
Safety & Licensing Technology
Atomic Energy of Canada Limited
2251 Speakman Dr.
Mississauga, Ontario, L5K 1B2
Canada
Popovn@aecl.ca

U.S. Rohatgi
Department of Advanced Technology
Brookhaven National Laboratory
Upton, New York, 11973
USA

H.E.C. Rummens and R.B. Duffey
Atomic Energy of Canada Limited
Chalk River Laboratories
Chalk River, Ontario, K0J 1J0
Canada

Abstract

Departure from nucleate boiling (DNB) and critical heat flux (CHF) in parallel-channel systems follow instability. Recent studies have demonstrated that instability in multiple channels precedes the limit of classic single channel (mass-flow controlled) CHF. A theory has been developed that can be used to predict the static (Ledinegg) instability in two-phase flow with constant pressure drop. Also, a non-dimensional form of the instability for natural circulation flow was derived. This paper is focused on the application of the flow instability theory to low-pressure forced circulation two-phase flow in vertical parallel annuli. The theory is used to understand and correlate the data collected from measurements of burnout power in vertical heated parallel annuli completed at Chalk River Laboratories (CRL), AECL, Canada. The paper provides a summary of recent developments of the stability theory, a brief description of single and parallel channel stability phenomena, a brief description of recent CRL experiments, and comparison of the results obtained using the CATHENA thermalhydraulics code and a simple analytical model.

Introduction

In parallel channel flow, the pressure drop, or the driving head for the flow, is maintained constant across any given channel by the flow in all other channels. This boundary condition is common in all heat exchangers, reactor cores and boilers. The two-phase flow in parallel vertical channels can exhibit both "static" and "dynamic" instabilities. The two-phase flow instability in vertical parallel channels under low pressure, which occurs following the Onset of Nucleate Boiling (ONB) and Onset of Significant Void (OSV), is essential in determining the point of Departure from Nucleate Boiling (DNB) and the Critical Heat Flux (CHF). The flow stability is studied to obtain a clear understanding of the mathematical tools that can be used in the reactor safety design and analysis to ensure that sufficient margin to burnout of reactor fuel elements is available.

In parallel heated channels, as the heat flux is increased, the coolant boils, and the two-phase produces an increase in the flow resistance. This leads to redistribution of the flow between the channels even while maintaining a constant pressure drop boundary conditions. For a forced flow system, the pressure drop is generally not constant, but is related to the flow rate, which may further affect the flow distribution.

Parallel vertical channel flow configuration is typical for small research reactors of high power density, such as the MAPLE reactor [Popov et.al., 1999]. A recent study [Cho et.al., 1999] concluded that annular fuel elements provide an optimal fuel design in small research reactors of high power density. The shape of the fuel elements requires coolant flow through the inside and outside annulus surrounding the fuel, thus creating a parallel flow configuration. In addition, many of these vertical fuel elements are located in the reactor core in separate flow channels, thus creating multiple parallel flow configuration.

A primary goal of the safety analysis is to demonstrate that there is a sufficient margin to DNB and local burnout during postulated events where there is a large mismatch between the fuel power and cooling capability. The need for understanding flow diversion or flow instability is to determine its effect on burnout and therefore on the impact in loss of safety margins.

In this paper, the flow stability methodology developed for vertical upward flow in parallel channels [Duffey et.al., 1990,

Rohatgi et.al., 1998], is applied to the recently obtained experimental data of vertical annular heater element burnout under subcooled low-pressure flow conditions.

The paper first describes the prediction of critical power for the fuel channel using the CATHENA code, followed by experimental data for similar electrically heated channels. In the last section, a simple method is described to estimate the scaling effects between the experimental and reactor conditions.

CATHENA is the primary AECL tool to perform safety analysis of CANDU and research nuclear reactors. The thermal-hydraulic model in CATHEHA [Hanna, 1998] uses a one-dimensional, non-equilibrium, two-fluid model similar to that found in other current state-of-the-art reactor analysis codes. The basic thermalhydraulic model consists of six partial differential equations for mass, momentum and energy conservation—three for each phase. The conservation equations are coupled by flow-regime dependent set of constitutive equations defining the transport of mass, momentum and energy between the phases and the walls. The gas phase may consist of a mixture of up to four noncondensable gas components and the vapour. The two-fluid thermalhydraulic model forms a set of coupled, non-linear, first-order partial differential equations with non-linear source terms. These equations are solved by idealising the thermalhydraulic network by a system of discrete control volumes. The thermalhydraulic finite-difference approximations of the partial differential equations are based on semi-implicit first-order, donor-cell upwind differencing over the control volumes. The resulting system matrix is solved by the Harwell MA28 sparse matrix solution subroutine library.

A generalised wall heat transfer package is used within CATHENA to model the heat transfer between the fluid and the wall. It includes the wall-to-fluid heat transfer (covering all flow boiling regimes), wall-to-wall heat transfer (including solid-solid wall heat transfer and radiation heat transfer), and heat conduction within a wall.

The CATHENA code includes component models such as pumps, valves, accumulator and generalised tank models, break discharge models and extensive control modelling capability. CATHENA approximates the core kinetics behaviour by that of a point reactor.

Nomenclature

a	constant in subcooled boiling expression, a = 38.4 for Saha-Zuber correlation.
A	Flow area, m^2
Cp	Specific heat, $kJ \cdot kg^{-1} \cdot °C^{-1}$
D	Hydraulic diameter, m
De	Equivalent diameter, m
f	Friction factor
G	Mass flux, $kg \cdot m^{-2} s^{-1}$
G_f	Ratio of mass flow rate, $(W_1/W_2)^2$
G_L	L/D Group
G_Q	Power ratio in channels, Q_2/Q_1
G_S	Stability Group
h_{fg}	Latent heat, $kJ \cdot kg^{-1}$
Δh_i	Inlet subcooling, $\Delta h_i = h_f - h_\ell$
k	Thermal conductivity, $kJ \cdot m^{-1} \cdot °C^{-1} \cdot s^{-1}$
$\overline{K}$	Non-dimensional loss coefficient, $\overline{K} = \frac{K}{N_{fr}}$
K_e	Exit loss coefficient
L	Length of heated section
N_f	Froude Number, $N_f = \frac{gL}{v^2}$
N_{fr}	Friction Number, $N_{fr} = \frac{fL}{2D}$
N_P	Phase Change Number, $N_p = \frac{Q\rho_\ell}{\left(Wh_{fg}\rho_g\right)}$
N_S	Subcooling Number, $N_s = \frac{\Delta h_i \rho_\ell}{\left(h_{fg}\rho_g\right)}$
Pe	Peclet number, $Pe = \mathrm{Re} \cdot \mathrm{Pr} = \frac{GD_e C_p}{k}$
Pr	Prandtl number
Re	Reynolds number
Q	Heat rate, kW
S	Flow split, $S = W_1 / W$
v	Velocity, $m \cdot s^{-1}$
W	Flow rate, $kg \cdot s^{-1}$
X_e	Exit equilibrium quality
Z_λ	Non-boiling length, m
ρ	Density, $kg \cdot m^{-3}$
σ	Surface tension, $N \cdot m^{-1}$

Subscripts

1	Inner channel
2	Outer channel
i	Inlet
e	Exit
f	Saturated liquid
g	Saturated vapor
l	liquid

Flow Instability Phenomena

Any flow system containing a heated channel is susceptible to instabilities, especially if there is void generation in the channel. The flow could have dynamic instability where the amplitude of the unstable part of the flow parameters will be function of time and may also grow. An example of such an instability is density wave instability. Similarly, in some situations the instability grows rapidly and behavior is governed by the static or steady state equations and it is called static instability or Leddineg Instability. This instability leads to flow excursion. The requirement for both type of instabilities is that in response to flow decrease or power increase, the increase in the pressure drop in the two-phase region will exceed the decrease in the pressure drop in the single phase region. The pressure drop for the channel will be inversely related to the flow, leading to unstable situation if the channel is subject to constant pressure drop boundary conditions. This can occur if the basic flow characterstic of boiling channels is as shown in Figure 1 for a vertical reactor channel.

In the case of multiple parallel channels, due to the pressure drop characterstic, the flow can redistribute and may lead to dryout in one of the channels. Small differences in initial flow and power distribution can lead to flow excursion as the channels approach the minimum pressure drop as shown in Figure 1.

The parallel channel phenomena and possible instabilities are investigated with experiments in an annular parallel channel setup and with analyses using the thermalhydraulic computer code CATHENA and simple models.

Single Channel Phenomena

The phenomenon of flow instability in a **single** channel is connected to the total channel pressure drop characteristics and supply pressure (see Figures 1 and 2 for an inner and outer channel calculated by the CATHENA code). The pressure drop in the channel is due to inlet loss, friction at the wall and the exit loss, with hydrostatic head changing with the void. The total pressure drop is a sum of single phase pressure drop including the entrance loss, and the two phase pressure drop including the exit loss in the channel.

In single-phase flow, as the flow decreases the pressure drop decreases very nearly with the square of the velocity (see Figures 1 and 2). However, as the flow decreases further, boiling first occurs at the exit of the channel, then extends upstream. The rate of decrease in the pressure drop slows down with the decrease in the flow as the density decreases due to vapour generation in the two-phase region. As the flow further decreases, void fraction increases, leading to an increase in the two phase pressure drop which applies to both the wall friction and the exit section. Once the void fraction increases beyond a certain point, the pressure drop starts to decrease again with the flow (frictional flow resistance with steam is less than with liquid). The maximum and the minimum of the characteristic curve depend upon the inlet subcooling, pressure, flow, and channel power.

The local dryout or overheating in a test channel will occur when conditions lead to either transition to high quality flow, where the water film on the surface dries out, or to very low flow or stagnation.

Figure 3 shows the impact of the exit losses in the inner and the outer heater channel respectively. The figure demonstrates that for the current setup the exit pressure loss does not have a significant impact on the slope of the pressure drop curve, nor on the point of minimum pressure drop. This leads to the conclusion that differences in exit losses do not have an important influence.

Parallel Channel Phenomena and CATHENA Analysis

The parallel channel phenomenon is more complex. The inner and the outer channels may have different cross-section areas, hydraulic diameters, flow resistance, power and flow. When channels with different geometry and flow conditions are operated in parallel, the two channels can undergo out-of-phase oscillations and flow diversion [Paniagua, et.al. 1999].

If the power is gradually increased in a two parallel channel system while keeping the inlet flow and subcooling fixed, the channels will first go into ONB and OSV. As the power is further increased beyond the OSV point, the flow in the channels may oscillate as a result of a churn and slug flow regime (especially at low mass flow rates), and flow diversion from one channel to the other may occur.

A similar behaviour is expected when the flow is gradually reduced and the power maintained constant. At some point during the flow decrease, the inner channel reaches the minimum point of the pressure drop characteristic first, thus leading to subsequent increase in the frictional pressure drop. This triggers a flow diversion from the inner channel into the outer channel, that may lead to local dryout. Therefore, as a first approximation, the metastable minimum and maximum point in the characteristic curve for the channel indicate the onset of flow diversion and dryout, respectively. However, it has been generally observed that heater burnout could also occur in the negative slope region between the minimum and maximum of the characteristic curve [Siman-Tov et. el., 1995].

Figure 4 shows a CATHENA calculation of the parallel channel flow behaviour during a slow reduction of the total

flow delivered to two annular parallel channels. The inlet coolant temperature in this calculation is 30°C, the total power is 50 kW, and the power split is 45.3/54.7% (inner/outer channel). Figure 4 demonstrates that first void is calculated in the inner channel because the heat flux is higher in the inner channel. As soon as a significant amount of void is calculated in the inner channel a rapid flow diversion from the inner to the outer channel is predicted. As a result of the flow diversion, the inner channel completely voids leading to burnout. The results in Figure 4 are obtained using the Saha-Zuber OSV model in CATHENA.

Figure 5 shows the impact of the power split, flow split and the exit flow resistance differences), obtained by CATHENA simulations. This figure confirms that the impact of the exit flow resistance of the inner channel is negligible when the flow split is kept unchanged. According to a CATHENA evaluation of the impact of the flow split, an 80% reduction of the exit losses in both channels leads in a 5% increase of the inner channel flow, that results in about 14% increase of burnout power. Note that the flow split is defined as the ratio of the flow in the inner channel to the flow in the outer channel in kg/s (the initial flow split is 38%/62%). Thus, an increase in the flow split means delivering more flow to the inner channel and less to the outer.

The impact of power split is the most significant parameter. As the power delivered to the inner channel increases (i.e., the normalized power split increases), the normalized burnout power decreases. Note that the power split is defined as the power delivered to the inner channel versus the power delivered to the outer channel (the initial power split is 45.33%/54.67%).

Figure 6 shows the impact of the local pressure on the flow diversion that leads to burnout. As expected, the behaviour shown in Figure 6 indicates a strong impact of the local pressure on the dryout power (also affects the bubble size). The local pressure affects the saturation temperature, which in turn affects the local subcooling at the dryout point. Subcooling is known to be a very important parameter that affects the CHF phenomenon.

The phenomena of parallel channel instability and dryout have been described and simulated with CATHENA code. In addition a set of experiments were also performed to verify the phenomena. They are described in the next section.

Brief Description of Experimental Facility and Data

Burnout experiments were performed using electrical heaters made of Inconel 718 to simulate annular fuel. As shown in Figure 7, the heater was cooled on both surfaces via an annular inner flow channel and an annular outer flow channel. The inner channel was formed by placing a central rod, electrically insulated, within the inner flow channel; the outer channel was constrained by a circular transparent poly-carbonate flow tube.

An inlet spacer kept the heater in position while allowin flow into the two channels. In the experiments, the spacer web at the inlet were also used to allow electrical current into the heater. At the outlet, the spacers were for alignment only; current exited via an extension of the heater and the inner channel flow exited via slots cut into that extension.

Alignment of the flow tube, heater, and center rod was of utmost importance because of the narrowness of the flow channels (~2 mm). O-rings were used in the assembly of the test-section to allow thermal expansion of the heater and thus avoid heater bowing.

Large currents were required to cause overheat, especially at high coolant flow rates. The power connections of the test section were therefore designed carefully to avoid electrical failure prior to heater burnout.

The burnout measurements were made at constant inlet temperature (30°C) and outlet pressure (~190 kPa A). The flow rate of the deionized water coolant was fixed during a test, and the electrical power increased slowly until the heater tubing reached critical heat flux (CHF) and overheated. This overheating resulted in heater failure due to the increased local electrical resistance, and hence defined the burnout condition for the heater.

The test-section and associated piping were enclosed within a tank with a transparent window. Burnout under the conditions of interest typically occurred quickly, severing the heater tube and breaking apart the test-section. For this reason, a tes section could not be re-used and yielded only one burnou point.

Figure 8 shows the burnout power for a single heater element, as a function of the total mass flow rate going through the test-section. Several other configurations are shown on the same graph: uniform heaters with a larger or smaller central rod, non-uniform heaters with a cosine-shaped axial power profile, and cluster-of-4 uniform heaters sharing the same flow tube. [In the latter case, the burnout power is per heater, as a function of the mass flow rate per heater.] The trend is linear, with certain data points below the line probably due to subtle misalignment of test components and hence premature burnout.

Comparison of the results revealed that the result differences between configurations could be explained solely by the differences in power split and flow split. The power split was obtained from heater resistance measurements, and the flow they was obtained from heat balance measurements and from independent pressure loss measurements. The burnout power appeared to be very sensitive to these splits; subchannel effects provided by cluster-of-4 tests seemed to be of lesser significance.

Video footage and visual observation revealed consistent flow patterns. Typically, as power was increased, the ONB occurred (characterized by a hissing sound from fine bubble collapse), followed by vapour bubbles streaming along the heater. With increasing heat, the vapour streams became thic opaque, and wavering, with a high enough void fraction suggest OSV (characterized by a rumbling or crackling sound

from the steady collapse of large void pockets). Once void coalescence and vapor blanketing was observed, the heater would typically glow orange and burn through.

Tests at high flow rates were characterized by very little visible void, as the bubbles were very small and traveling rapidly; burnout took fractions of a second. Tests at low flow rates were characterized by large bubbles and plenty of visible void; burnout would be preceded by slug flow, with slugs appearing intermittently at first and more regularly with the addition of heat. Burnout was visibly connected with local liquid depletion and vapour blanketing over the heater surface.

Test analysis showed that the more extreme channel (according to channel power and flow rate), i.e., the channel with the greater void fraction, was consistently the first to experience burnout. From observation, we deduced that burnout was precipitated by diversion of flow away from the higher-void (more extreme) channel as the system attempted to maintain a pressure balance in the parallel system.

Further evidence of pressure balancing was given in the lowest-flow test. Under these conditions, the buoyancy of a vapour pocket became significant compared to the obstruction pressure loss, which helped to draw fluid back into the more highly voided, depleted channel. Because the heat flux was also low, the heater could survive the temporary flow depletion, and slugs were seen alternating between the two channels.

Scaling Flow-Instability in Vertical Annuli

The tests described previously indicated that there was sudden burnout of the heaters by flow excursion. To apply the heater burnout data to reactor conditions, a simple scaling analysis was performed.

The maximum and minimum of the pressure drop characteristic curves discussed earlier depend upon inlet subcooling, pressure, flow, power, the normalized inlet and exit loss coefficients (to a lesser extent), and the gravity terms. There are six scaling parameters for this phenomenon for each channel: Subcooling Number (N_s), Phase Change Number (N_p), Friction Number (N_{fr}), Froude Number (N_f), and normalised inlet and exit loss coefficients (K_i and K_e).

Using first order equilibrium flow instability theory [Rohatgi, et. al. 1998], it is useful to show the burnout data on the N_p-N_s plot, which provides a good tool for comparison of burnout data from different sources. Figure 9 shows the burnout data compared to data from other sources. The range of burnout test conditions were N_p ~ 35 to 100, and N_s ~ 80 to 150. Some data in Figure 9 were obtained in single channel facilities, whereas the CRL heater burnout data (dark circles) were obtained in a parallel channel configuration. Figure 9 illustrates that some of the single-channel data are clustered around the $N_p=N_s$ line, whereas most of the data are clustered around the $N_p=0.7 \cdot N_s$ line. The CRL burnout data are very close to the $N_p=0.5 \cdot N_s$ line, which indicates a burnout at a lower power (for the same subcooling) than the other data used for comparison. The possible reason for this difference is channel asymmetry.

Appendix A provides the details of the model that is used to scale the CRL burnout data. Six groups of parameters are identified that are required to scale the CRL burnout data. The most important effects are represented in G_Q, G_f and G_s. G_f determines the flow split, G_s represents a measure of the severity of flow oscillations, and G_Q indicates the power split. Thus, G_Q and G_f are indicators of the effect on the parallel channel phenomena, and G_s is an indicator of the flow oscillation for an individual channel.

The most important differences between the CRL burnout test conditions and the reactor conditions with respect to local dryout are:

- the two-channel vs multi-channel configuration in the core (the bypass effect),
- the flow split due to different loss coefficients and flow areas,
- power split, and
- local pressure.

The impact of these differences is evaluated in this section using the model described in Appendix A.

A bypass channel with an area exceeding four times the area of the hot channel is sufficient to model the bypass effect of a large core. The effect of a bypass is that the burnout occurs closer to the flow diversion point, which is assumed to take place at the point of ΔP_{min} on the ΔP/Flow curve. Tests also showed that at low pressures even with a bypass channel with an area equal to the area of the hot channel, the burnout occurred close to the point of ΔP_{min} which is a characteristic of large bypass. The burnout tests were done with two channels in parallel (the inner and outer heater channel). As shown in Figures 1 and 2, the ΔP_{min} points for two channels are close. The flow redistribution just before the burnout is expected to be small, leading to a smaller change in pressure in each channel. Therefore, the system will behave essentially as a constant pressure drop system. The second channel provides a means to redistribute the flow in response to the increase in pressure drop in the voided channel. Based on this analysis, and the analysis presented in Appendix A, CHF in the CRL burnout tests is expected to be near the ΔP_{min} point (in terms of the power-cooling mismatch) and the difference in the flow bypass between the burnout tests and the reactor conditions is expected to be negligible.

The CRL burnout tests have larger differences in flow restriction (or K's) between the two channels than the reactor fuel channels, with the inner channel in the tests receiving lower flow and thus being susceptible to burnout at lower power. Therefore, in the tests, the inner channel power at burnout is expected to be lower. The power ratio indicates that the outer channel has larger power fraction in the burnout test than the

fuel channel, indicating that the outer channel will be susceptible to burnout at lower total power. The non-dimensional number G_s for both channels in the burnout tests is lower, indicating the possibility of burnout at a lower power. The combined effect of these two differences on the critical power can be estimated based on the flow split. First, the flow split is estimated, and then the combined effect with the power split is calculated.

The flow split is calculated using the typical reactor conditions:

$$S = \frac{\left(G_f\right)^{0.5}}{\left(1+G_f^{0.5}\right)} = 0.47 \qquad (1)$$

Since two different K distributions among the inner and outer channels were used in the test, the flow split will have the following range:

$$S = 0.37 - 0.43 \qquad (2)$$

Therefore, the critical power ratio between the test and the reactor representation, based on the Saha-Zuber OSV correlation (assuming that the OSV point defines the point of flow diversion and therefore burnout), is

$$\frac{[N_P]_{reactor}}{[N_P]_{CRL}} = \frac{\left((1+G_Q)d\,S\right)_{reactor}}{\left((1+G_Q)d\,S\right)_{CRL}} = 1.09 - 1.21 \qquad (3)$$

This model is based on the assumption of uniform heating in the burnout tests.

The results of this analysis are also illustrated in Figures 10 to 13. Figure 10 shows the effect of the exit loss coefficient on the inner channel burnout power. The solid line represents the results obtained for the heater using simple calculations with the Saha-Zuber OSV model (which is conservatively used in this model as an indicator to burnout). The dotted line represents the calculation for the reactor conditions. As expected, this effect is small, and it decreases with the flow.

Figure 11 shows a comparison of the burnout data in the heater and for reactor conditions (analyses for the inner channel CHF), and it includes the power split and the flow split. The difference is larger as the flow increases, and this figures indicates that burnout data under-represent the power at burnout for reactor conditions. Figure 12 shows a comparison when the burnout is assumed in the outer channel. In this case, the burnout data over-represent the burnout power for reactor conditions.

Figure 13 summarizes the results for the inner and the outer channel. The difference between the cases when burnout is assumed in the inner or the outer channel is much larger in the burnout tests than is expected for the reactor conditions.

The difference in the exit loss coefficient makes the power at burnout in the heater tests up to 5% lower than in the actual in-reactor conditions.

The combined effect of the flow split and the power split depends on the channel that dries out first. If the inner channel is assumed to dry out first, then the measured power in the heater tests is lower by up to 21% than the power at local dryout for the in-reactor conditions.

If the outer channel is assumed to dry out first, the measured power at burnout in the heater tests is higher by up to 11% than the power for the reactor conditions. The total power calculated assuming burnout in the outer channel is always higher than the calculated power for burnout in the inner channel. Therefore, it is less likely that the outer channel will burnout before the inner channel (this is also supported by the CATHENA analysis presented earlier). Furthermore, in the actual reactor conditions, there is heat loss out of the outer channel that is not represented in the burnout tests, making burnout of the outer fuel sheath less likely.

The above estimates of the impact of differences between the burnout test conditions and the reactor conditions are based on a conservative assumption that burnout will occur at or very near to the onset of instability, i.e., near the point of minimum ΔP vs. flow curve (which is near OSV for that channel). However, not all flow oscillations lead to burnout.

The difference in the inlet pressure is also identified to be scaled. The burnout tests were performed at an outlet pressure of 180-200 kPa (a). The fuel elements in the reactor core are at outlet pressure of about 180 kPa (a). The difference in the inlet pressure between the tests and the reactor conditions is up to 100 kPa. In the burnout tests performed with uniform axial power profile, the local pressure at the burnout location (end of the heated part) was higher than the pressure at the test section outlet as a result of higher exit losses in the tests compared to the reactor conditions.

To evaluate the effect of pressure in the tests, calculations were performed using the model described in Appendix A. This analysis assumed that the inlet temperature and the flow are fixed. Figure 14 shows a comparison of the total burnout power for the cases where only water properties were changed because of the change in the inlet pressure from 200 to 500 kPa(a), and the cases where the inlet subcooling is changed as a result of the change in the inlet pressure. The figure also shows that the impact of the change in water properties is small compared to the effect of the change in the inlet subcooling as a result of the pressure change. It is evident that the impact of the inlet pressure (for fixed inlet temperature and flow) is significant. For example, a change in the inlet pressure of 100 kPa at flow of 1.5 $kg \cdot s^{-1}$ results in a change of the burnout power by about 15%. Figure 15 shows the effect of inlet pressure in the Np-Ns domain. Figure 15 demonstrates that using the N_P/N_S ratio as function of flow from burnout tests eliminates the need for scaling the inlet pressure. This is expected because the Saha-Zuber correlation along with the flow and power split are not a strong function of pressure. The only significant effect is expected for Pe< 70,000 through the Reynolds and Prandtl numbers. Also the figure shows that

ratio decreases as flow increases and then stabilises. This trend is due to the Pe number effect in the Saha-Zuber correlation.

Summary and Conclusions

This paper presents an integrated approach of predicting burnout for an annular parallel channel system, using the thermal-hydraulic code CATHENA, and using a simple scaling analyses. A brief description of burnout tests using annular heaters is also presented. The following conclusions are drawn from the test data and the model predictions:

1. Burnout in the parallel channel system occurs due to flow diversion from one channel to the other. The flow diversion generally occurs around the minimum in the pressure drop - flow characteristic curve.
2. Six scaling parameters can be conveniently chosen to capture the differences between the heater test conditions and the in-reactor conditions. These parameters are: Subcooling Number (N_s), Phase Change Number (N_p), Friction Number (N_{fr}), Froude Number (N_f), and normalized inlet and outlet loss coefficients (K_i and K_e).
3. In case of parallel channel system the initial flow split is the most important parameter in determining the burnout power.
4. The system pressure has insignificant effect on burnout power for the same inlet subcooling.
5. The inlet subcooling has a significant effect on the burnout power.
6. The relationship between the Phase Change number (Zuber number) based on burnout power and inlet subcooling provides a general relationship for predicting burnout power.
7. A simple method is presented that scales the burnout power from the tests to the reactor conditions.

References

Cho, D-K., Kim, M-H., and Sohn, D-S., 1999, "Nuclear Design Methodology of Fission Moly Target for Research Reactor", Journal of the Korean Nuclear Society, Volume 31, No. 4, pp.365-374.

Duffey, R.B., and Hughes, E.D., 1990, "Static Flow Instability Onset in Tubes, Channels, Annuli, and Rod Bundles", ASME Conference on 'Thermalhydraulics of Advanced Nuclear Reactors', Book No. G00547.

Hanna, B.N., 1998, "CATHENA: A Thermalhydraulic Code for CANDU Analysis", Nuclear Engineering and Design, Vol. 180, pp.113-131.

Paniagua, J, et al., 1997, "Thermal Hydraulic Instabilities during Start-up in Two Heated Parallel Channels", ASME Winter Annual Meeting, Dallas, Texas.

Popov, N.K., Lee, A.G., Langman, V. , 1999, "Application of the CATHENA Thermalhydraulics Code to MAPLE Research Reactor Safety Analysis", CNS Conference, Montreal, Quebec, Canada.

Rohatgi, U.S. and Duffey, R.B., 1998, "Stability, DNB, and CHF in Natural Circulation Two-Phase Flow", Int. Comm. Heat and Mass Transfer, Vol. 25, No. 2, pp. 161-174.

Siman-Tov, M., Felde, D.K., McDuffee, J.L. and Yoder, G.L., 1995, "Static Flow Instability in Subcooled Flow Boiling in Parallel Channels", 2nd International Conference on Multiphase Flow '95, Kyoto, Japan, April 3-7.

Appendix A:

Model Formulation for Scaling of Heater Burnout Data

The objective of this model is to provide a tool for estimating the quantitative impact of scale differences described in the paper. To calculate the effect of scale differences, only the important effects are modelled in the flow field.

The effect of the exit losses on the single channel flow instability is bracketed by the following criteria, based on first order equilibrium flow instability theory [Rohatgi et al., 1998]:

$$N_P \geq N_S \qquad \text{(A-1)}$$

$$N_P/N_S = ((2+K_e)+(K_e^2+K_e+1)^{1/2})/(1+K_e) \qquad \text{(A-2)}$$

Equation (A-2) can be used to evaluate the impact of the exit losses on the dryout behaviour of a single channel in terms of N_p-N_s criteria.

The parallel channel dryout behaviour is characterised by flow diversion from one channel to the other. The local dryout always occurs in the channel with the reduced flow, while the other channel experiences an increased flow and could well be in a single-phase liquid flow regime. However, the total flow to the heater, and the total pressure drop, are fixed. The flow split, S, is related to flow parameters such as power and friction coefficients. The flow split is calculated by equating the pressure drops in the two channels, assuming that the potential burnout channel has two-phase conditions and the other channel is in liquid phase. A steady momentum balance equation between the channels consist of friction and gravity terms.

$$S^2\left[N_{fr1}\left[\frac{Z_{\lambda 1}}{L}+\left(1-\frac{Z_{\lambda 1}}{L}\right)\frac{\rho_l}{\rho_{md}}+\frac{\overline{K}_{il}}{2}+\frac{\overline{K}_{el}}{2}+\frac{\overline{K}_{el}\rho_l}{\rho_{md}}\right]\right] \qquad \text{(A-3)}$$

$$= (1-S)^2\left(\frac{A_1}{A_2}\right)^2\left[N_{fr2}\left[1+\frac{\overline{K}_{i2}}{2}+\frac{\overline{K}_{e2}}{2}\right]\right]$$

$$+\left(\frac{\frac{A_1}{A_2}}{1+\frac{A_1}{A_2}}\right)^2\left(\frac{gLA^2\rho_l^2}{W^2}\right)\left(1-\frac{Z_{\lambda 1}}{L}\right)\frac{\rho_{ma1}}{\rho_{l1}}$$

Equation (A-3) has two unknowns, Z_λ, the non-boiling length, and exit quality which determines the exit and average densities in the two-phase region. These variables depend upon subcooled boiling phenomena. Local dryout occurs at the exit of uniformly heated channel and it is close to the OSV. Equation (A-3) can be simplified as follows:

$$S^2\left[Nfr1\left[\frac{Ns}{Npl}+\left(1-\frac{Ns}{Npl}\right)\left(1+\frac{Npl-Ns}{2}\right)+\frac{\overline{K}_{il}}{2}+\frac{\overline{K}_{el}}{2}+\frac{\overline{K}el}{2}\left(\frac{\rho_g}{\rho_e}\right)(Npl-Ns)\right]\right]$$

$$= (1-S)^2\left(\frac{A_1}{A_2}\right)^2\left[N_{fr2}\left[1+\frac{\overline{K}_{i2}}{2}+\frac{\overline{K}_{e2}}{2}\right]\right]$$

$$+\left(\frac{\frac{A_1}{A_2}}{1+\frac{A_1}{A_2}}\right)^2\left(\frac{gLA^2\rho_l^2}{W^2}\right)\left(1-\frac{N_s}{N_{pl}}\right)\left(\frac{1}{1+(N_{pl}-N_s)\left(\frac{\rho_g}{\rho_l}\right)}\right) \quad \text{(A-4)}$$

$$S=\frac{W_1}{W} \quad \text{(A-5)}$$

Therefore, Equation (A-4) indicates that the flow split depends on the following parameters:

$$S=f\left(N_s, N_{pl}, N_{fr1}, N_{fr2}, \overline{K}_{i1}, \overline{K}_{e1}, \overline{K}_{i2}, \overline{K}_{e2}, \left(\frac{\rho_g}{\rho_l}\right), \left(\frac{A_1}{A_2}\right), N_f\right) \quad \text{(A-6)}$$

It is conservative to assume that a heated channel will reach an unstable state (minimum in ΔP versus Flow; see Figure 9), even when $N_{p1}<N_s$ due to subcooled boiling. A criterion for the OSV, which defines the onset of flow instability, can be used as a conservative indicator of burnout. The OSV can be obtained from the Saha-Zuber correlation for subcooled boiling and is given here as:

$$N_{p1}=\frac{N_s}{\left(1+\frac{a}{L/D}\right)} \quad \text{(A-7)}$$

$a = 38.4 \cdot P_e/70{,}000$ for $Pe < 70{,}000$

$a = 38.4$ for $Pe \geq 70{,}000$

The Saha-Zuber OSV model is easy to use and has the correct general trend. Also since the objective is to compar test conditions (using heaters) with the in-reactor conditions using the same correlation for both involves the same systematic bias, and any difference in the prediction of power at the flow instability (i.e., dryout) is due to scale difference alone.

Based on the simple models described with Equation (A-4), the non-dimensional groups which need to be matched between the heater and the actual fuel channel can be defined. The list of non-dimensional groups is given in the expression for the flow split, i.e., Equation (A-6), along with Peclet number and L/D.

The heater burnout tests provided an average power, total flow rate and inlet subcooling at burnout conditions. An expression for the average power, when one channel (inner channel) is assumed to burn out is given by:

$$Q = Q_1 + Q_2 = Q_1 \cdot (1+G_Q) \quad \text{(A-8)}$$

where G_Q is the ratio of the power to the outer and the inner channel (Q_2/Q_1).

From the Saha-Zuber criterion, Equation (A-7), an expression for total power for given flow rate and subcooling can be derived as follows:

$$Q_1 = N_S \cdot W_1 h_{fg} \frac{\left(\frac{\rho_g}{\rho_l}\right)}{\left(1+\frac{a}{L/D_1}\right)} \qquad \text{(A-9)}$$

For convenience, the following parameter can be defined:

$$d = \frac{1}{\left(1+\frac{a}{(L/D_1)}\right)} \qquad \text{(A-10)}$$

The total power for the heater burnout test section can be obtained from the burnout power of one channel, the flow split and the power split. The total power is the sum of the power to the individual channels. The net N_P will be between Ns for two channels.

$$Q = (1+G_Q)\cdot d\cdot N_S\cdot S\cdot W\cdot h_{fg}\cdot(\rho_g/\rho_l) \qquad \text{(A-11)}$$

$$\langle N_P\rangle = (1+G_Q)\cdot d\cdot S\cdot N_S \qquad \text{(A-12)}$$

For the flow conditions observed in the heater burnout tests (except for very low flow), the friction terms are an order of magnitude larger than the gravity terms. The Froude number is also small. For low Froude number, small exit quality X_e and $N_{pl}\approx N_s$, the initial flow split is obtained from Equation (A-4):

$$\left(\frac{S}{1-S}\right)^2 = \left(\frac{A_1}{A_2}\right)^2 \frac{N_{fr2}}{N_{fr1}} \frac{\left(1+\frac{\overline{K}_{i2}}{2}+\frac{\overline{K}_{e2}}{2}\right)}{\left(1+\frac{\overline{K}_{i1}}{2}+\frac{\overline{K}_{e1}}{2}\right)} \qquad \text{(A-13)}$$

With the above simplifications, the number of dimensionless groups needed for scaling decreases to four. However, if the burnout occurs in the other channel, a fifth group is required that deals with the geometry of the other channel. Thus, the reduced set of five non-dimensional groups are as follows:

$$G_Q = \frac{Q_2}{Q_1}, GL_1 = \frac{L}{D_1}, N_s, GL_2 = \frac{L}{D_2}$$

$$G_f = \left(\frac{A_1}{A_2}\right)^2 \left(\frac{Nfr2}{N_{fr1}}\right) \frac{\left(1+\frac{\overline{K}_{i2}}{2}+\frac{\overline{K}_{e2}}{2}\right)}{\left(1+\frac{\overline{K}_{i1}}{2}+\frac{\overline{K}_{e1}}{2}\right)}, \qquad (A-14)$$

Equation (A-2) provides the sixth group which indicates the severity of the flow instability, and it is referred to as G_s, where $G_s=N_{pl}/N_s$.

Ideally, these groups should be matched between the heater burnout tests and the reactor conditions. If there are scale differences between the tests and the reactor conditions, an estimate of the bias in the critical power due to the scale differences has to be made. Note that the effect of the Reynolds number has been neglected.

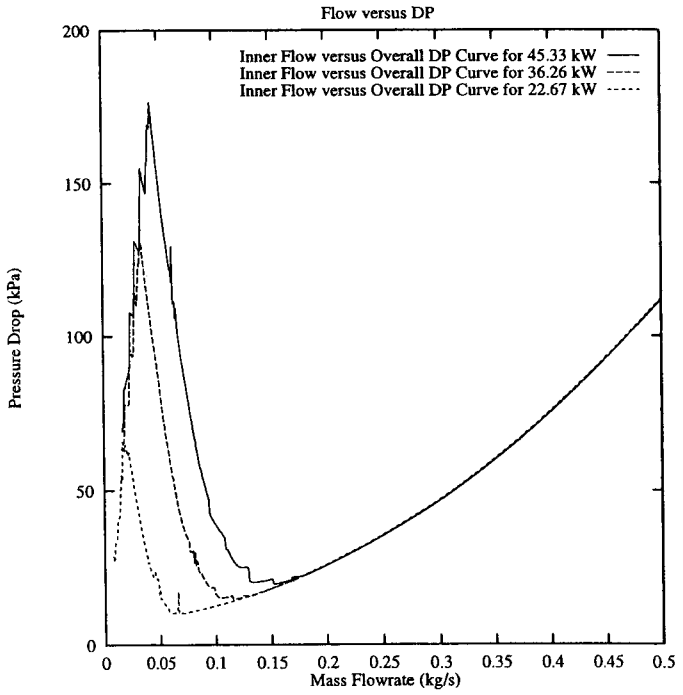

Figure 1: Pressure Drop Characteristics of the Heater Inner Channel Calculated by CATHENA

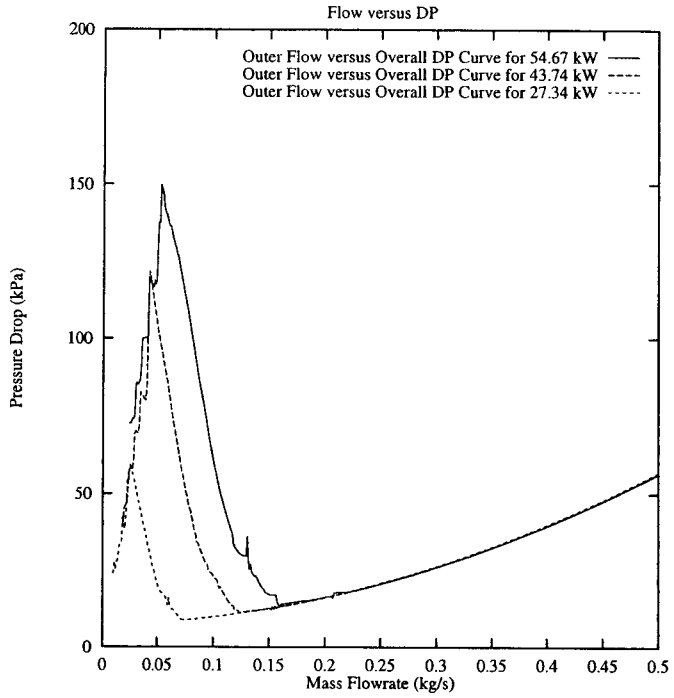

Figure 2: Pressure Drop Characteristics of the Heater Outer Channel Calculated by CATHENA

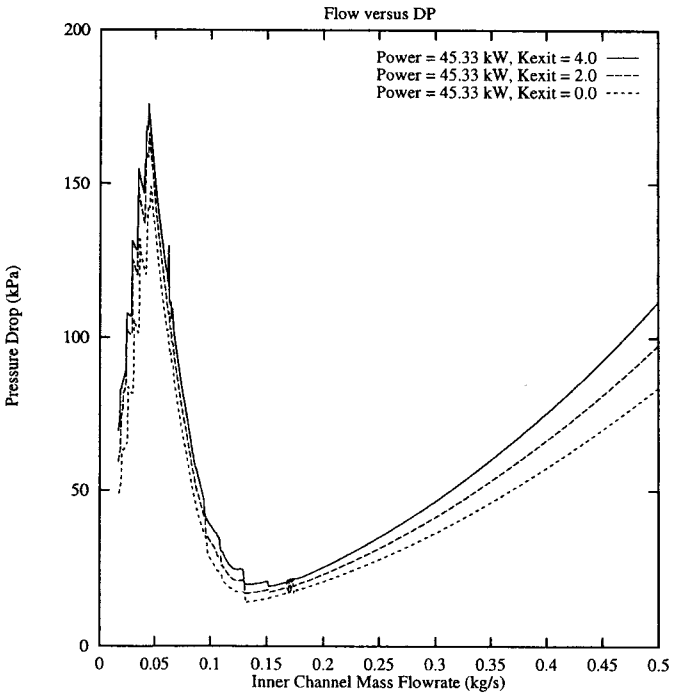

Figure 3: Effect of Exit Losses on Pressure Drop Characteristics of the Heater Inner Channel Calculated by CATHENA

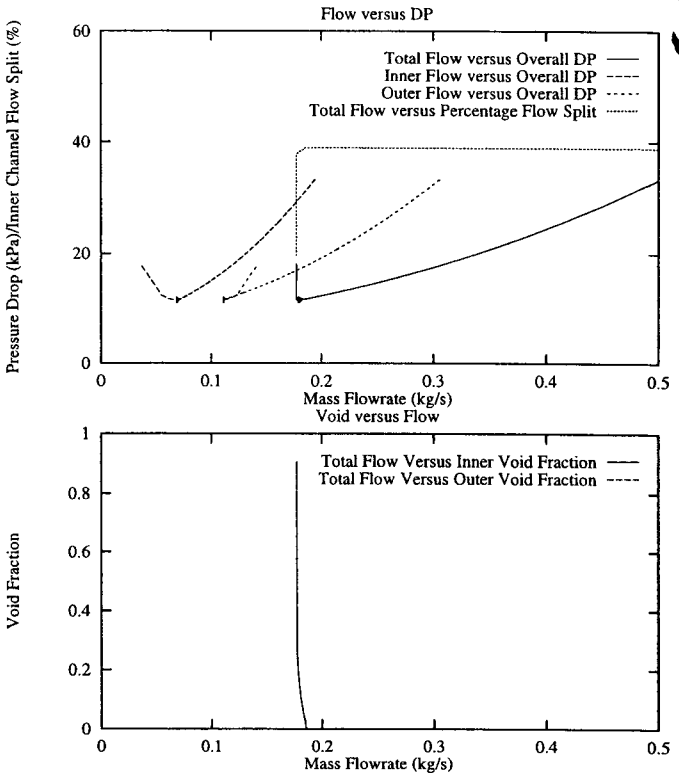

Figure 4: Pressure Drop Characteristics of the Heater Calculated by CATHENA (Inner and Outer Channel Combined)

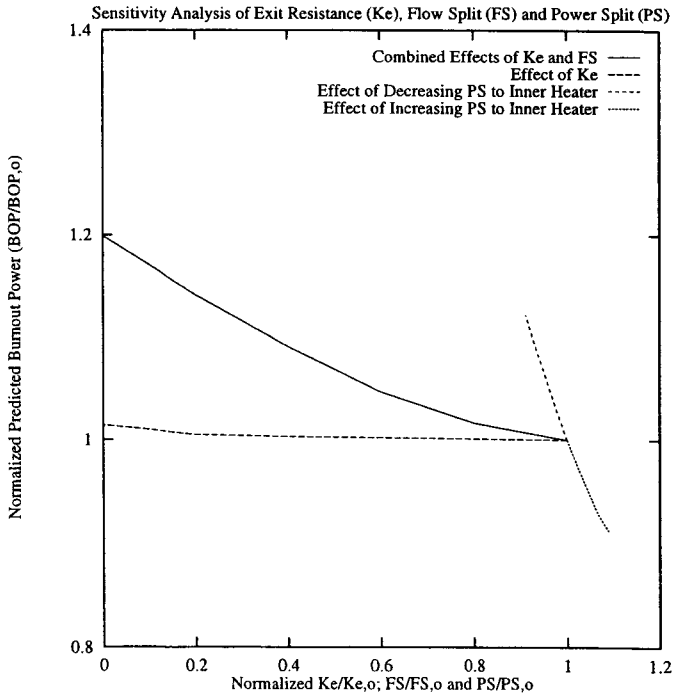

Figure 5: Effect of Power Split, Flow Split and Exit Flo Resistance on Burnout Power Calculated by CATHENA Using P2CHF-3 Burnout Test

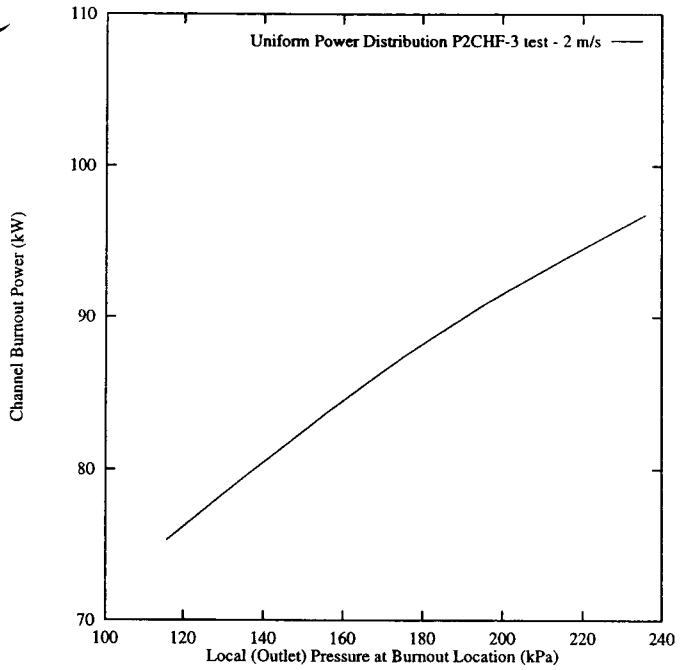

Figure 6: The Effect of Local Pressure on Predicted Burnout Power in Heater Burnout Tests Calculated by CATHENA

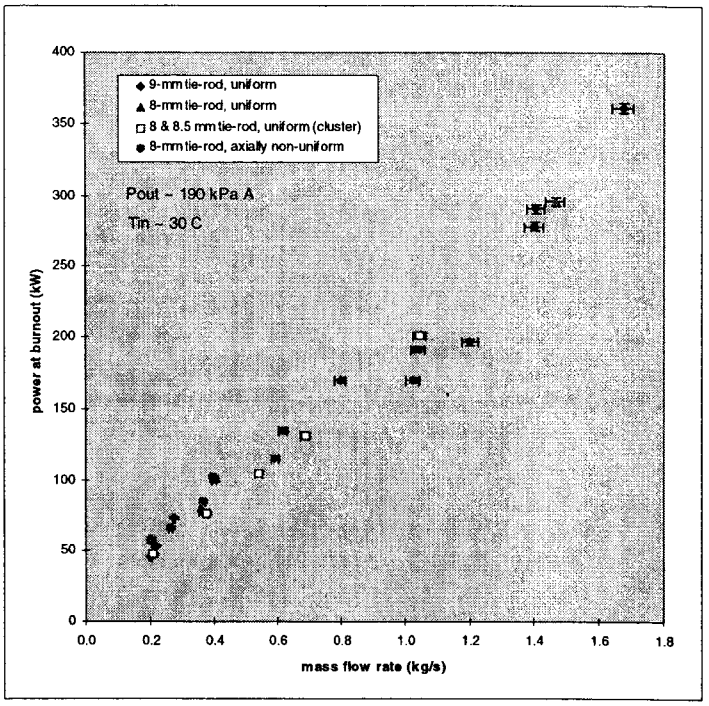

Figure 8: Power at burnout as a function of mass flow rate, for a single heater element.

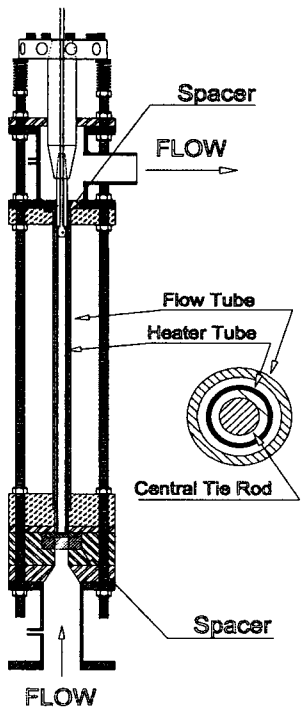

Figure 7: Schematic of single-heater test-section

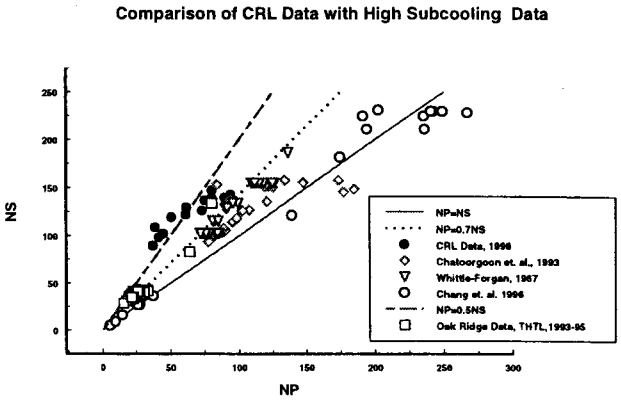

Figure 9: Comparison of Heater Burnout Data with Other High Subcooling Low Pressure Data

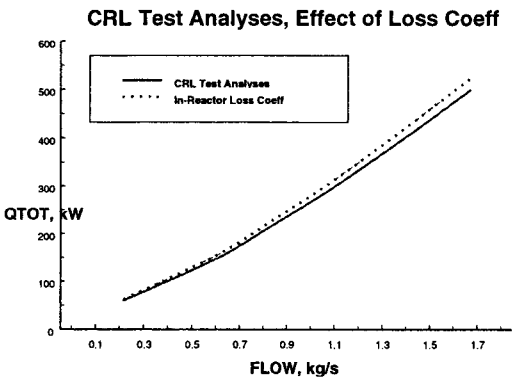

Figure 10: The Effect of the Exit Loss Coefficient (Using the Model Described in Appendix A)

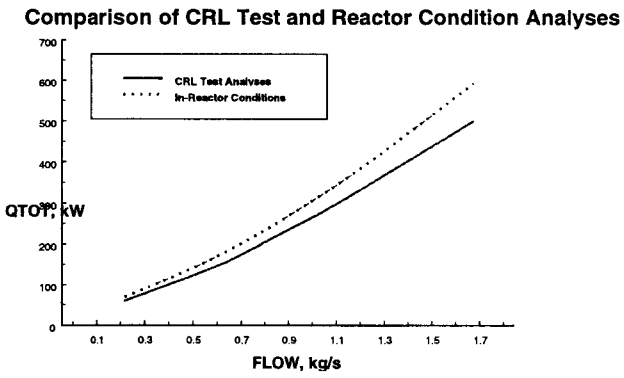

Figure 11: Inner Channel Analysis (Using the Model Described in Appendix A)

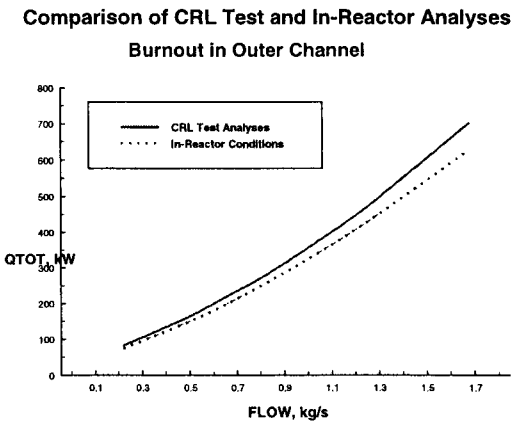

Figure 12: Outer Fuel Channel Analysis (Using the Model Described in Appendix A)

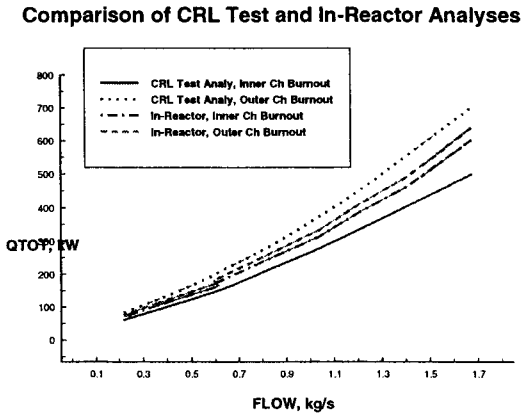

Figure 13: Summary of Inner and Outer Channel Analysis (Using the Model Described in Appendix A)

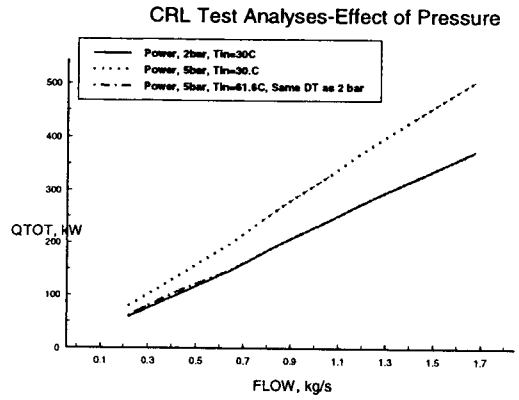

Figure 14: The Effect of Local Pressure on Local Subcooling and Coolant Properties (Using the Model Described in Appendix A)

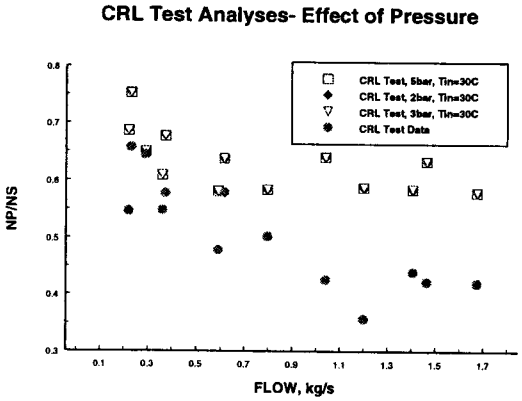

Figure 15: The Effect of Local Pressure in the Np-Ns Domain (Using the Model Described in Appendix A)